Inorganic Chemistry

ARTICLE

pubs.acs.org/IC

Role of Anions and Reaction Conditions in the Preparation of Uranium(VI), Neptunium(VI), and Plutonium(VI) Borates

Shuao Wang,[†] Eric M. Villa,[†] Juan Diwu,[†] Evgeny V. Alekseev,[†,‡] Wulf Depmeier,[‡] and Thomas E. Albrecht-Schmitt*[,†]

[†]Department of Civil Engineering and Geological Sciences and Department of Chemistry and Biochemistry, University of Notre Dame, 156 Fitzpatrick Hall, University of Notre Dame, Notre Dame, Indiana 46556, United States

[‡]Institut für Geowissenschaften, Universität zu Kiel, 24118 Kiel, Germany

Supporting Information

ABSTRACT: U(VI), Np(VI), and Pu(VI) borates with the formula $AnO_2[B_8O_{11}(OH)_4]$ (An = U, Np, Pu) have been prepared via the reactions of U(VI) nitrate, Np(VI) perchlorate, or Pu(IV) or Pu(VI) nitrate with molten boric acid. These compounds are all isotypic and consist of a linear actinyl(VI) cation, AnO_2^{2+}, surrounded by BO_3 triangles and BO_4 tetrahedra to create an AnO_8 hexagonal bipyramidal environment. The actinyl bond lengths are consistent with actinide contraction across this series. The borate anions bridge between actinyl units to create sheets. Additional BO_3 triangles and BO_4 tetrahedra extend from the polyborate layers and connect these sheets together to form a three-dimensional chiral framework structure. UV−vis−NIR absorption and fluorescence spectroscopy confirms the hexavalent oxidation state in all three compounds. Bond-valence parameters are developed for Np(VI).

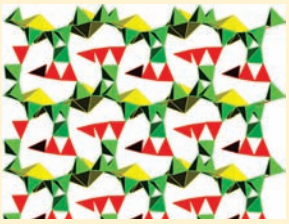

INTRODUCTION

The terrestrial abundance of boron, and therefore borates, is quite low at 10 ppm.[1] However, borate deposits occur as the result of the evaporation of ancient oceans and seas. One such deposit is the Salado formation near Carlsbad, New Mexico where the concentration of borate, predominately in the form of H_3BO_3, $B(OH)_4^-$, and $B_4O_7^{2-}$, reaches concentrations as high as 166 ppm in intergranular brines.[2] Located within this deposit is the United States' only repository for nuclear defense waste known as the Waste Isolation Pilot Plant (WIPP). Much like boron, uranium has a relatively low terrestrial abundance at 2.7 ppm.[3] However, a variety of processes concentrate uranium in the Earth's crust, and large deposits of uranium are found throughout the world. Despite the fact that vast quantities of uranium are dissolved in oceans and seas, there are no known naturally occurring uranium borate minerals that form as the result of evaporation of ancient bodies of water.[4] WIPP presents a unique environment whereby large quantities of not only uranium, but also lesser amounts of the transuranium elements neptunium, plutonium, americium, curium, will eventually be able to react with the brines, potentially leading to the formation of actinide borate compounds. The presence of the decaying nuclear waste will lead to heating beyond the ambient conditions in the deposit, and therefore the reaction of actinides with borates at moderate temperatures (ca. 150 °C) are important reactions to study to predict the fate of actinides in the repository.

The structural chemistry of both borates and actinides is very rich. Borate occurs as both BO_3 triangles and BO_4 tetrahedra, and these units fuse in limitless combinations to create clusters, chains, sheets, and three-dimensional frameworks of remarkable complexity.[5] Likewise, the coordination chemistry of actinides is exceedingly rich with tri- and tetravalent actinide cations being found with coordination numbers ranging from 6 to 15,[6] and penta- and hexavalent actinide cations forming the ubiquitous linear actinyl units, AnO_2^{n+} (An = U, Np, Pu, Am; n = 1 or 2), that are further ligated by four to six donor groups to create tetragonal, pentagonal, and hexagonal bipyramids.[7] The combination of the structural flexibility of actinides with borates should lead to countless novel materials, some of which will have relevance to the disposition and fate of nuclear waste. Despite these motivations, the first uranyl borate for which a crystal structure is known was not reported until 1985, when Behm disclosed the remarkable structure of $K_6[UO_2\{B_{16}O_{24}(OH)_8\}]\cdot 12H_2O$, an extraordinarily complex cluster composed of a cyclic BO_3 and BO_4 units with a central uranyl core.[8] This work was quickly followed by that of Gasperin, who utilized high-temperature B_2O_3 melts to prepare seven different uranyl borates, one of which contains an early example of uranyl cations using oxo atoms to coordinate one another, a so-called cation−cation interaction.[9−15] For 20 years the field lay dormant until the use of boric acid flux reactions was introduced providing access to thorium,[16,17] uranium,[18−21] neptunium,[22−24] and plutonium[22] borates with both unprecedented structural richness and complex electronic structures.

One of the challenges in working with these elements is to find synthetic methods that allow for isolation of single oxidation states across a series of neighboring actinides (e.g., U(VI), Np(VI), Pu(VI)).[25] This can be difficult to achieve because the redox potentials for uranium, neptunium, and plutonium are very different, and plutonium is well-known to equilibrate as many as four different oxidation states in solution at the same time.[26] Concentration,[27]

Received: November 25, 2010
Published: February 03, 2011

temperature,[28] counterions,[29] radiolysis,[30] and hydrolysis[31] can all significantly alter the course of reactions involving actinides. If proper conditions can be created for preparing a series of actinide compounds with the same formula and oxidation state, systematic comparisons of these compounds can be made.

We have recently discovered that molten boric acid is a unique medium for preparing crystalline actinide borates. We have reported a large family of U(VI) borates, many of which adopt noncentrosymmetric structures.[18−21] In a boric acid flux Np(V) partially disproportionates to Np(IV) and Np(VI) allowing for the isolation of neptunium borates, such as $K_4(NpO_2)_{6.73}B_{20}O_{36}(OH)_2$ and $K_2[(NpO_2)_3B_{10}O_{16}(OH)_2(NO_3)_2]$, that simultaneously contain three different oxidation states.[22,23] Lowering the reaction temperature and changing the flux to methyl boronic acid allows for the isolation of a neptunium borate, $NpO_2[B_3O_4(OH)_2]$, that only contains Np(V).[24] When Pu(VI) is reacted with molten boric acid the hexavalent oxidation state is maintained, and we have briefly communicated the synthesis and structure of $PuO_2[B_8O_{11}(OH)_4]$.[22]

In this work we will show how anions present in the reactions influence the formation of neptunium and plutonium borates. We demonstrate that by judicious choice of counterions and careful control of reaction conditions that a series of uranium, neptunium, and plutonium borates can be synthesized that all contain actinides in the hexavalent oxidation state allowing for the development of periodic trends.

EXPERIMENTAL SECTION

Syntheses. $UO_2(NO_3)_2 \cdot 6H_2O$ (98%, International Bio-Analytical Industries), H_3BO_3 (99.99%, Alfa-Aesar), $Pb(NO_3)_2$ (99%, Alfa-Aesar), and KBO_2 (Alfa-Aesar) were used as received. Reactions were run in PTFE-lined Parr 4749 autoclaves with a 23 mL internal volume for uranium, and with 10 mL internal volume autoclaves for neptunium and plutonium. Distilled and Millipore filtered water was used in all reactions. Standard precautions were performed for handling radioactive materials during work with thorium and uranium.

Caution! *^{237}Np ($t_{1/2} = 2.14 \times 10^6$ y) represents a serious health risk owing to its α and γ emission, and especially because of its decay to the short-lived isotope ^{233}Pa ($t_{1/2} = 27.0$ d), which is a potent β and γ emitter. ^{242}Pu ($t_{1/2} = 3.76 \times 10^5$ y) represents a serious health risk owing to its α and γ emission. All studies with neptunium and plutonium were conducted in a laboratory dedicated to studies on transuranium elements. This laboratory is located in a nuclear science facility and is equipped with a HEPA filtered hoods and negative pressure gloveboxes that are ported directly into the hoods. A series of counters continually monitor radiation levels in the laboratory. The laboratory is licensed by the Nuclear Regulatory Commission. All experiments were carried out with approved safety operating procedures. All free-flowing solids are worked with in gloveboxes, and products are only examined when coated with either water or Krytox oil and water. There are significant limitations in accurately determining yield with neptunium and plutonium compounds because this requires drying, isolating, and weighing a solid, which poses certain risks, as well as manipulation difficulties given the small quantities employed in the reactions.*

A stock solution of $^{237}Np(VI)$ perchlorate was prepare by first digesting NpO_2 in 8 M HNO_3 for 3 days at 200 °C (in an autoclave). The solution was reduced to a moist residue and redissolved in water forming a Np(VI) nitrate solution. A large excess of $NaNO_2$ followed by an excess of NH_4OH were added to this solution resulting in the precipitation of Np(V) hydroxide. The precipitate was then filtered and dried in 120 °C for about 30 min. Np(V) hydroxide was then dissolved in a dilute $HClO_4$ solution. This solution was then ozonated with an Ozonology ozone generator for approximately 1 h to ensure complete oxidation of the neptunium to +6. UV−vis−NIR spectroscopy indicated that only Np(VI) was present.

A stock solution of $^{242}Pu(VI)$ nitrate was prepare by first digesting PuO_2 in 8 M HNO_3 for 3 days at 200 °C (in an autoclave). The solution was reduced to a moist residue and redissolved in water. This solution was then ozonated for approximately 5 h to ensure complete oxidation of the plutonium to +6. UV−vis−NIR spectroscopy indicated that only Pu(VI) was present. A stock solution of $^{242}Pu(IV)$ nitrate was made by treating $^{242}Pu(VI)$ nitrate stock solution with small excess of H_2O_2 followed by mild heating.

$UO_2[B_8O_{11}(OH)_4]$. $UO_2(NO_3)_2 \cdot 6H_2O$ (0.5000 g, 1 mmol), boric acid (1.3596 g, 22 mmol), $Pb(NO_3)_2$ (0.3317 g, 1 mmol), and water (50 μL) were loaded into a 23 mL autoclave. The autoclave was sealed and heated to 220 °C in a box furnace for 500 h. The autoclave was then cooled down to room temperature at a rate of 5 °C/h. The products were washed with boiling water to remove excess boric acid, followed by rinsing with methanol. Crystals in the form of tablets with light yellow-green coloration were collected for $UO_2[B_8O_{11}(OH)_4]$ as a minor phase. β−$UO_2B_2O_4$ (**UBO-1**) was also found as the main product.[19]

$NpO_2[B_8O_{11}(OH)_4]$. A stock solution of Np(VI) perchlorate containing 20 mg of Np(VI) perchlorate was loaded into a 10 mL autoclave and dried in the oven at 120 °C until the whole solution appeared to be a drop (about 20 μL in volume). Boric acid (0.094 g, 1.5 mmol) and KBO_2 (0.0154 g, 0.18 mmol) were then added to the autoclave. The autoclave was sealed and heated to 220 °C in a box furnace for 3 days. The autoclave was then cooled down to room temperature at a rate of 9 °C/h. The products were washed with boiling water to remove excess boric acid, followed by rinsing with methanol. Crystals in the form of tablets with light peach-pink coloration were collected for $NpO_2[B_8O_{11}(OH)_4]$ as the only product.

$PuO_2[B_8O_{11}(OH)_4]$. A stock solution of Pu(VI) nitrate containing 10 mg of Pu(VI) nitrate was loaded into a 10 mL autoclave and dried in the oven at 120 °C until the whole solution appeared to be a drop (about 20 μL in volume). Boric acid (0.0472 g, 0.7 mmol) was then added to the autoclave. The autoclave was sealed and heated to 220 °C in a box furnace for 3 days. The autoclave was then cooled down to room temperature at a rate of 9 °C/h. The products were washed with boiling water to remove excess boric acid, followed by rinsing with methanol. Crystals in the form of tablets with peach-pink coloration were collected for $PuO_2[B_8O_{11}(OH)_4]$ as a pure product.

Crystallographic Studies. Single crystals of all three $UO_2[B_8O_{11}(OH)_4]$, $NpO_2[B_8O_{11}(OH)_4]$, and $PuO_2[B_8O_{11}(OH)_4]$ phases were mounted on cryoloops with viscous Krytox and optically aligned on a Bruker APEXII CCD X-ray diffractometer or a Bruker APEXII Quazar X-ray diffractometer using a digital camera. Initial intensity measurements were either performed using a IμS X-ray source, a 30 W microfocused sealed tube (MoKα, $\lambda = 0.71073$ Å) with high-brilliance and high-performance focusing Quazar multilayer optics, or a standard sealed tube with a monocapillary collimator. Standard APEXII software was used for determination of the unit cells and data collection control. The intensities of reflections of a sphere were collected by a combination of four sets of exposures (frames). Each set had a different φ angle for the crystal, and each exposure covered a range of 0.5° in ω. A total of 1464 frames were collected with an exposure time per frame of 10 to 30 s, depending on the crystal. The SAINT software was used for data integration including Lorentz and polarization corrections. Semiempirical absorption corrections were applied using the program SADABS.[32]

UV−vis−NIR and Fluorescence Spectroscopy. UV−vis−NIR data were acquired from single crystals of all phases using a Craic Technologies microspectrophotometer. Crystals were placed on quartz slides under Krytox oil, and the data was collected from 400 to 1400 nm. Fluorescence data were obtained using 365 nm light for excitation (see Supporting Information).

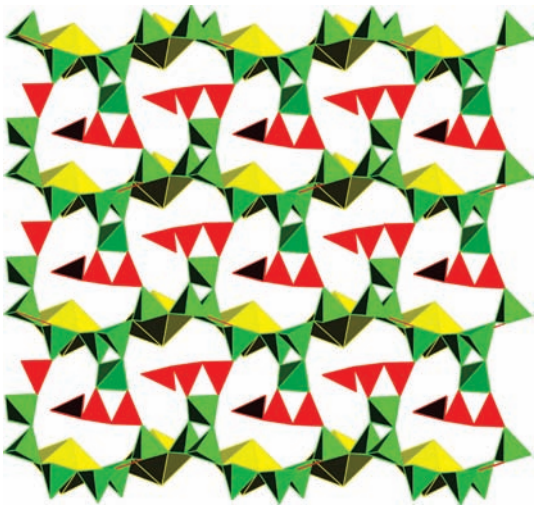

Figure 1. Depiction of the noncentrosymmetric, three-dimensional network structure found for $AnO_2[B_8O_{11}(OH)_4]$ (An = U, Np. Pu). AnO_8 hexagonal bipyramids are shown in yellow, BO_3 triangles in red, and BO_4 tetrahedra in green.

Figure 2. View along the *b* axis of the actinyl borate sheets in $AnO_2[B_8O_{11}(OH)_4]$ (An = U, Np, Pu). AnO_8 hexagonal bipyramids are shown in yellow, BO_3 triangles in red, and BO_4 tetrahedra in green.

RESULTS AND DISCUSSION

Controlling the Oxidation States of Neptunium and Plutonium Borates. In our previous report, we described the syntheses of $K_4(NpO_2)_{6.73}[B_{20}O_{36}(OH)_2]$ and $Ba_2(NpO_2)_{6.59}[B_{20}O_{36}(OH)_2]\cdot H_2O$, which contain Np(IV), Np(V), and Np(VI).[22] These compounds are synthesized by the reactions of Np(VI) nitrate with molten boric acid. When chloride is the only counterion in the reaction $(NpO_2)_4[(NpO_2)_{6.73}B_{20}O_{36}(OH)_2]$ forms.[22] This demonstrates that Np(VI) is first reduced to Np(V) followed by disproportionation. We noted, however, that when Np(VI) perchlorate is heated in water at 200 °C that initially Np(V) grows into the reaction, but that after prolonged heating the neptunium is predominately in the +6 oxidation state. Perchlorate is in fact a strong oxidant; it simply has a large kinetic barrier for reacting. Presumably these high temperatures are overcoming that barrier. Likewise, when Np(VI) perchlorate is reacted with molten boric acid, the first Np(VI) borate, $NpO_2[B_8O_{11}(OH)_4]$ is isolated.

The reaction chemistry of plutonium in boric acid is much more straightforward than with neptunium. Both Pu(IV) and Pu(VI) nitrate react with boric acid to yield $PuO_2[B_8O_{11}(OH)_4]$. Unlike uranyl and neptunyl borates, additional cations are not readily incorporated into the structure. $PuO_2[B_8O_{11}(OH)_4]$ also crystallizes in the presence of Ba^{2+} and K^+. The isolation of a Pu(VI) borate from a Pu(IV) source is surprising in light of the fact that Pu(IV) compounds are generally far less soluble than Pu(VI) compounds.[26]

The isolation of an uranium analogue of the aforementioned Np(VI) and Pu(VI) compounds, $UO_2[B_8O_{11}(OH)_4]$, requires the use of higher temperatures than we have typically employed in uranyl borate syntheses. At 190 °C an entirely different set of compounds forms that possess very different polyborate networks.[18−21] However, by increasing the reaction temperature to 220 °C, $UO_2[B_8O_{11}(OH)_4]$ can be isolated.

Structure and Topology Description. Single crystal X-ray diffraction studies of $UO_2[B_8O_{11}(OH)_4]$, $NpO_2[B_8O_{11}(OH)_4]$, and $PuO_2[B_8O_{11}(OH)_4]$ show that $AnO_2[B_8O_{11}(OH)_4]$ crystal structures are all isotypic and crystallize in the noncentrosymmetric monoclinic space group *Cc*. A view of the overall structure is shown in Figure 1. There is one crystallographically unique actinyl cation, AnO_2^{2+}, that resides in a hexagonal hole within the polyborate sheets to create a hexagonal bipyramidal environment, AnO_8. This coordination environment dominates the entire family of actinyl borates derived from molten boric acid, and is a consequence of having small chelating anions. Similar environments can be found with other small chelating anions such as nitrate and carbonate.[7a] This coordination environment is actually quite rare in extended structures when compared with the prevalence of AnO_7 pentagonal bipyramids that are found in 85% of actinyl compounds.[7a]

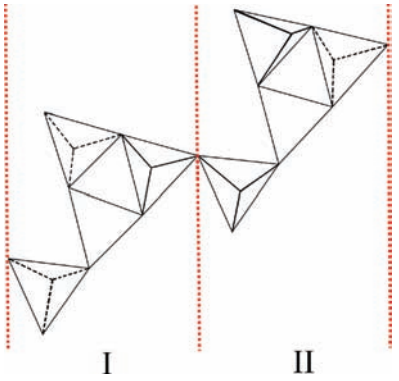

Figure 3. Skeletal view of the actinyl borate sheets in $AnO_2[B_8O_{11}(OH)_4]$ (An = U, Np, Pu). Solid-line tetrahedra directed "up", dashed-line "down".

Each AnO_8 unit is surrounded by nine borate groups in the [*ac*] plane to form an actinyl borate sheet as shown in Figure 2. Among these nine borate groups, there are two BO_3 triangles and seven BO_4 tetrahedra. The terminal oxygen of five BO_4 tetrahedra are directed "up"/"down" corresponding to the sheet plane and other two are directed in the opposite "down"/"up" direction. This is the same number of surrounding BO_3 triangles and BO_4 tetrahedra we found in **C**/**D** and **E** types of uranyl borate sheets which were observed in Tl-uranyl borates.[18] However, the topology of the layers in the new U, Np, and Pu borates is different, and has not been seen in any other actinide borate that

dx.doi.org/10.1021/ic102356d |*Inorg. Chem.* 2011, 50, 2527–2533

Table 1. Crystallographic Data for $UO_2[B_8O_{11}(OH)_4]$, $NpO_2[B_8O_{11}(OH)_4]$, and $PuO_2[B_8O_{11}(OH)_4]$

	$UO_2[B_8O_{11}(OH)_4]$	$NpO_2[B_8O_{11}(OH)_4]$	$PuO_2[B_8O_{11}(OH)_4]$
mass	596.51	595.48	600.48
color and habit	light yellow-green, tablet	pale pink, tablet	peach-pink, tablet
space group	*Cc*	*Cc*	*Cc*
a (Å)	6.4476(15)	6.4426(8)	6.4391(8)
b (Å)	16.741(4)	16.705(2)	16.714(2)
c (Å)	10.964(3)	10.9843(13)	10.9648(13)
β (deg)	90.675(2)	90.766 (1)	90.744(1)
V (Å^3)	1183.4(5)	1182.1(2)	1180.0(3)
Z	4	4	4
T (K)	100(2)	100(2)	100(2)
λ (Å)	0.71073	0.71073	0.71073
maximum 2θ (deg)	28.53	27.58	28.79
ρ calcd (g cm^{-3})	3.348	3.346	3.38
μ (Mo Kα)	138.27	89.02	56.97
$R(F)$ for $F_o^2 > 2\sigma(F_o^2)$[a]	0.0300	0.0247	0.0205
$Rw(F_o^2)$	0.0612	0.0531	0.0473

[a] $R(F) = \sum||F_o| - |F_c||/\sum|F_o|$.

Table 2. Selected Bond Distances for $AnO_2[B_8O_{11}(OH)_4]$ (An = U, Np, Pu)

	distance (Å)						
	An = U	An = Np	An = Pu		An = U	An = Np	An = Pu
An(1)−O(3)	1.733(5)	1.737(5)	1.720(4)	B(1)−O(5)	1.470(11)	1.462(10)	1.459(9)
An(1)−O(10)	1.767(5)	1.746(5)	1.733(4)	B(1)−O(6)	1.472(12)	1.471(11)	1.464(10)
An(1)−O(7)	2.405(7)	2.399(13)	2.399(11)	B(1)−O(11)	1.472(12)	1.474(15)	1.505(10)
An(1)−O(6)	2.436(8)	2.440(9)	2.438(7)	B(1)−O(7)	1.478(12)	1.479(11)	1.479(13)
An(1)−O(2)	2.468(6)	2.468(5)	2.454(4)	B(2)−O(2)	1.348(12)	1.352(10)	1.352(9)
An(1)−O(8)	2.529(7)	2.527(13)	2.527(10)	B(2)−O(1)	1.368(11)	1.371(10)	1.347(9)
An(1)−O(5)	2.532(7)	2.544(8)	2.527(6)	B(2)−O(6)	1.382(12)	1.363(11)	1.385(10)
An(1)−O(1)	2.622(6)	2.639(5)	2.634(4)	B(3)−O(8)	1.424(11)	1.457(14)	1.452(13)
				B(3)−O(7)	1.428(11)	1.444(14)	1.437(11)
				B(3)−O(2)	1.490(10)	1.470(9)	1.466(8)
				B(3)−O(12)	1.533(11)	1.510(10)	1.526(8)
				B(4)−O(5)	1.409(11)	1.397(12)	1.409(10)
				B(4)−O(8)	1.422(11)	1.379(16)	1.403(13)
				B(4)−O(1)	1.454(10)	1.411(10)	1.456(9)
				B(4)−O(4)	1.583(13)	1.755(15)	1.601(11)
				B(5)−O(15)	1.425(13)	1.523(14)	1.444(12)
				B(5)−O(9)	1.454(13)	1.389(13)	1.424(11)
				B(5)−O(4)	1.498(13)	1.473(16)	1.535(13)
				B(5)−O(12)	1.515(13)	1.538(14)	1.516(11)
				B(6)−O(11)	1.329(12)	1.307(14)	1.320(11)
				B(6)−O(9)	1.357(12)	1.334(13)	1.342(10)
				B(6)−O(13)	1.408(12)	1.439(15)	1.430(11)
				B(7)−O(15)	1.323(15)	1.329(15)	1.301(12)
				B(7)−O(13)	1.388(14)	1.391(13)	1.387(11)
				B(7)−O(14)	1.398(15)	1.340(15)	1.415(12)
				B(8)−O(14)	1.341(18)	1.25(2)	1.388(14)
				B(8)−O(17)	1.411(19)	1.52(2)	1.428(16)
				B(8)−O(16)	1.417(19)	1.40(2)	1.333(17)

we have observed.[11−17] The basic fragment of the borate sheets is shown in Figure 3. It consists of two symmetrical parts **I** and **II** related via a mirror reflecting in the sheet plane. Such configuration makes layers in these new phases nonpolar, and we call this sheet type as **H**-type (relatively to sheets classifications of uranyl borates).[18−21]

dx.doi.org/10.1021/ic102356d |*Inorg. Chem.* 2011, 50, 2527–2533

Table 3. Results from the Calculation of Bond-Valence Parameters

compound	CN	S	ICSD
$Cs_2(NpO_2(SO_4)_2)$	7	5.99	51501[37a]
$(NpO_2)(CrO_4)(CO(NH_2)_2)_2$	7	5.94	93940[37b]
$NH_4(NpO_2)(NO_3)_3$	8	6.06	95921[37c]
$K(NpO_2)(NO_3)_3$	8	6.12	95922[37c]
$(NpO_2)_2(TcO_4)_4(H_2O)_3$	7	6.15	98417[37d]
	7	6.06	
$((CH3)_4N)_4(NpO_2(CO_3)_3)(H_2O)_8$	8	5.97	110324[37e]
$K(NpO_2)(PO_4)(H_2O)_3$	6	6.02	157297[37f]
$Na(NpO_2)(PO_4)(H_2O)_3$	6	6.06	157298[37f]
$Rb(NpO_2)(PO_4)(H_2O)_3$	6	5.79	157299[37f]
$NH_4(NpO_2)(PO_4)(H_2O)_3$	6	5.91	157300[37f]
$Na_{14}(Na_2(NpO_2)_2(GeW_9O_{34})_2)(H_2O)_{37}$	7	5.76	173174[37g]
$NpO_2(CH_3PO_3)$	7	6.02	173370[37h]
$(NpO_2)(SO_4)_2(H_2SO_4)(H_2O)_4$	7	5.94	201192[37i]
$Rb(NpO_2)(NO_3)_3$	8	6.08	201232[37j]
$K_2(NpO_2)_2(CrO_4)_3(H_2O)_4$	7	6.23	250164[37k]
	7	6.22	
$(NpO_2)(IO_3)_2(H_2O)$	7	5.90	281463[37l]
$(NpO_2)(IO_3)_2(H_2O)$	7	5.92	281464[37l]
$K(NpO_2)(IO_3)_3(H_2O)_{1.5}$	7	6.10	413240[31m]
$(NpO_2)(IO_3)_2(KCl)_{0.5}(H_2O)_{3.25}$	7	6.16	413331[31n]
$NpO_2(C_2H_5PO_3)$	7	5.80	
$NpO_2(B_8O_{11}(OH)_4)$	8	5.86	this work

There are additional BO_3 triangles and BO_4 tetrahedra connecting these actinyl borate sheets together, and the sheets stack along the *b* axis to form a three-dimensional framework structure. On the basis of the classification of actinyl borates these structures can be described as **F-2-2** compounds.[21] It should be noted that this is the only actinyl borate structure type from boric acid reactions where BO_4 tetrahedra are located between the sheets.[18−23] As indicated by the space group *Cc*, the structure is noncentrosymmetric, and this can be understood by the helical nature of the polyborate chains between the actinyl borate sheets. The twisting of the interlayer borate groups with respect to one another reduces the interlayer space, and yields a less open, denser structure.

The actinide contraction in this series of compounds can be demonstrated with a variety of metrics. The unit cell parameters given in Table 1 and the bond distances provided in Table 2 all provide evidence of this.

The unit cell volumes for $UO_2[B_8O_{11}(OH)_4]$, $NpO_2[B_8O_{11}(OH)_4]$, and $PuO_2[B_8O_{11}(OH)_4]$ are 1183.4(5) Å^3, 1182.1(2) Å^3, and 1180.0(3) Å^3, respectively. More importantly the actinyl An≡O bond distances shrink by 0.02 Å on average from uranium to plutonium. The Np≡O bond distances are within normal range and compare well with the neptunyl bond distance found in the $[NpO_2(NO_3)_3]^-$, which also contain neptunium in an hexagonal bipyramidal environment.[33] There are very few plutonyl crystal structures; far too few to make broad comparisons. However, the average Pu≡O bond length in $PuO_2[B_8O_{11}(OH)_4]$ is within 3σ of the plutonyl bonds in $PuO_2(IO_3)_2\cdot H_2O$.[34] It is important to note that actinyl bond distances are close enough to each other across the uranium, neptunium, and plutonium series that the actinide contraction is difficult to detect between different types of compounds (i.e., the errors in the bond lengths produce overlap if one uses 3σ on the calculated errors). The actinide contraction is only detectable if the errors are small, the residuals are low, and the compounds are isostructural.[35]

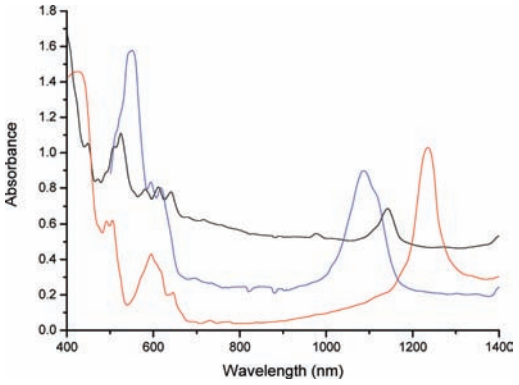

Figure 4. UV−vis−NIR absorption spectra of the Np(VI) compounds, $NpO_2[B_8O_{11}(OH)_4]$ (black), $NpO_2(NO_3)_2\cdot 6H_2O$ (blue), and $NpO_2(IO_3)_2(H_2O)$ (red).

Bond-Valence Parameters for Neptunium(VI). The bond valence parameters for Np^{6+} were derived before the 1970s;[36] however, as more and more structures of Np^{6+} have been reported it is important to improve on the original parameters using the 23 structures in total found in ICSD (Table 3)[37] and synthesized by us. To derive the values of R_0 and *b* at the same time for Np^{6+} neptunyl polyhedra, it is critical to establish the ideal bond distance of the neptunyl ions which corresponds to 2.0 *v.u.* (valence units). Burns and co-workers have derived the bond-valence parameters for U^{6+} and Np^{5+} using this method.[7b,38] Here, taking only well refined anhydrous structures into consideration, the bond strengths of the neptunyl bonds were calculated by subtracting the bond valence of other bonds to a given neptunyl O ion using the published parameters[39] from the formal valence of 2.0 for O, and then plotted as a function of the bond length. The intercept of the linear fit for these points corresponding to the ideal distance is 1.717 Å (R^2 = 0.9948). Thus, the relationship between R_0 and *b* follows the equation below:

$$2.0 = \exp[(R_0 - 1.717) / b]$$

With this constraint, the values of R_0 = 2.025 and *b* = 0.444 are obtained by optimizing the values to give the bond valence sum of 6.0 *v.u.* for 23 compounds. The results are shown in Table 3. This set of parameters works very well for most compounds giving an average bond valence sum of 6.00 *v.u.*, and the standard deviation is 0.13 *v.u.*, while the previous reported parameters of R_0 = 2.07 and *b* = 0.35 give the completely unreasonable average bond-valence sum of 7.12 *v.u.* and the standard deviation 0.21 *v.u.*

UV−vis−NIR Absorption Spectroscopy. The $5f^1$ electron configuration typically yields a single somewhat broad Laporte-forbidden f-f transition in addition to higher energy charge-transfer bands.[40] For U(V) the f-f transition is in the visible region of the spectrum.[40] For isoelectronic Np(VI), this transition occurs in the NIR near 1200 nm. The UV−vis−NIR spectra of $NpO_2[B_8O_{11}(OH)_4]$ acquired from a single crystal is shown in Figure 4. We have found that this peak can be shifted from where it typically occurs in solution when compared to solid samples. For example, data acquired from single crystals of $NpO_2(NO_3)_2\cdot 6H_2O$ shows this peak is located at 1100 nm. $NpO_2[B_8O_{11}(OH)_4]$ shows a transition at 1140 nm. In contrast,

dx.doi.org/10.1021/ic102356d |*Inorg. Chem.* 2011, 50, 2527–2533

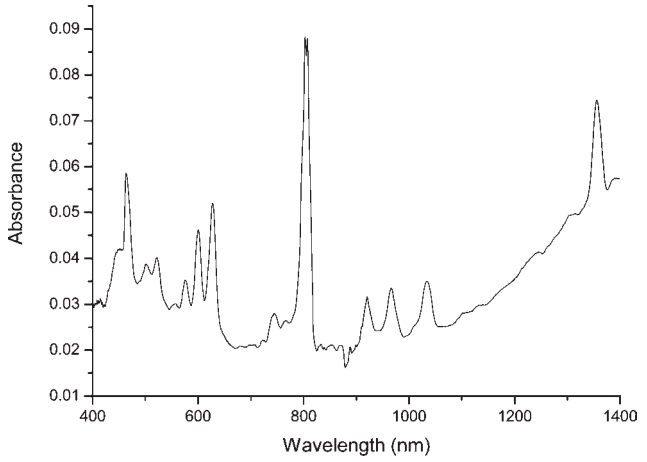

Figure 5. UV−vis−NIR absorption spectrum of $PuO_2[B_8O_{11}(OH)_4]$ from a single crystal aligned along the *b* axis in the same direction as the plutonyl units.

in single crystals of $NpO_2(IO_3)_2(H_2O)$ the transition is at 1230 nm, which is similar to where it is found in perchlorate and nitrate solutions.[41] An partial explanation for the differences in the energy of this transition is found in the coordination environments. In $NpO_2[B_8O_{11}(OH)_4]$ and $NpO_2(NO_3)_2\cdot 6H_2O$ the neptunium center is in a hexagonal bipyramidal environment; whereas in $NpO_2(IO_3)_2(H_2O)$ and solutions of neptunyl perchlorate the neptunium is in a pentagonal bipyramidal geometry.[25] It appears that the addition of a larger number of donor atoms in the equatorial plane, and presumably more electron density at the neptunium center, shifts the f-f transition to higher energy. The reverse effect is observed in the shift of the main transition at 980 nm in Np(V) compounds. Upon the formation of cation−cation interactions, the f-f transition shifts to longer wavelengths.[42]

Pu(VI) yields a spectrum that is far more complex than Np(VI) because of its $5f^2$ electron configuration. Superficially the spectrum is similar to isoelectronic Np(V) with a single strong f-f transition at approximately 830 nm. A series of much weaker transitions also occur. The UV−vis−NIR spectrum of single crystals of $PuO_2[B_8O_{11}(OH)_4]$ is shown in Figure 5. This spectrum was acquired from a single crystal where the plutonyl axis is aligned in the excitation direction. The main f-f transition is at 800 nm.[40] However if the crystal is rotated by 90° so that excitation is perpendicular to the plutonyl axis then the intensity of this transition is significantly diminished with respect to all of the other transitions. This pleochroism can be significant in other transuranium compounds, such as $K_2[(NpO_2)_3B_{10}O_{16}(OH)_2(NO_3)_2]$,[23] and is visible to the naked eye without polarized light. Crystals of both $PuO_2[B_8O_{11}(OH)_4]$ and $PuO_2(IO_3)_2\cdot H_2O$ are dichroic being pink when viewed in one direction and peach in the other two directions.

CONCLUSIONS

In summary, we have successfully synthesized the first Np(VI) borate in molten boric acid by using Np(VI) perchlorate as the starting material. This compound has uranium and plutonium analogues that are accessible by carefully controlling the reaction conditions. The actinide contraction can be detected in this system because of the high quality of the X-ray diffraction data even though all of the crystals are pseudomerohedrally twinned. Bond-valence parameters for Np(VI) have been developed that when used in conjunction with Np(IV)[43] and Np(V)[7b,44] parameters derived by us and others can be used to rapidly and accurately determine the oxidation state(s) of neptunium from the crystal structure alone. UV−vis−NIR data acquired from single crystals demonstrates that there can be substantial shifts in the f-f transitions when solids with one coordination environment are compared with solutions containing actinides in a different coordination environment. Taken together these data provide a series of general tools that illuminate differences between solution and the solid state for actinide compounds.

ASSOCIATED CONTENT

Supporting Information. Fluorescence spectra for $UO_2[B_8O_{11}(OH)_4]$; X-ray files (CIF) for $UO_2[B_8O_{11}(OH)_4]$, $NpO_2[B_8O_{11}(OH)_4]$, and $PuO_2[B_8O_{11}(OH)_4]$. This material is available free of charge via the Internet at http://pubs.acs.org.

AUTHOR INFORMATION

Corresponding Author
*E-mail: talbrec1@nd.edu. Fax: (+01)574-631-9236.

ACKNOWLEDGMENT

We are grateful for support provided by the Chemical Sciences, Geosciences, and Biosciences Division, Office of Basic Energy Sciences, Office of Science, Heavy Elements Program, U.S. Department of Energy, under Grants DE-FG02-01ER16026 and DE-SC0002215. This material is based upon work supported as part of the Materials Science of Actinides, an Energy Frontier Research Center funded by the U.S. Department of Energy, Office of Science, Office of Basic Energy Sciences under Award Number DE-SC0001089.

REFERENCES

(1) Nakano, T.; Nakamura, E. *Phys. Earth Planet. Inter.* **2001**, *127*, 233.
(2) Snider, A. C. *Verification of the Definition of Generic Weep Brine and the Development of a Recipe for This Brine*; ERMS 527505. Sandia National Laboratories: Carlsbad, NM, 2003.
(3) Taylor, S. R. *Geochim. Cosmochim. Acta* **1964**, *28*, 1273.
(4) Burns, P. C.; Grice, J. D.; Hawthorne, F. C. *Can. Mineral.* **1995**, *33*, 1131.
(5) (a) Yuan, G.; Xue, D. *Acta Crystallogr.* **2007**, *B63*, 353. (b) Grice, J. D.; Burns, P. C.; Hawthorne, F. C. *Can. Mineral.* **1999**, *37*, 731.
(6) (a) Daly, S. R.; Piccoli, P. M. B.; Schultz, A. J.; Todorova, T. K.; Gagliardi, L.; Girolami, G. S. *Angew. Chem., Int. Ed.* **2010**, *49*, 3379. (b) Orlova, A. I. *Structural Chemistry of Inorganic Actinide Compounds*; Elsevier: Amsterdam, The Netherlands, 2007; Chapter 8, p 315.
(7) (a) Burns, P. C. *Can. Mineral.* **2005**, *43*, 1839. (b) Forbes, T. Z.; Wallace, C.; Burns, P. C. *Can. Mineral.* **2008**, *44*, 1623.
(8) Behm, H. *Acta Crystallogr.* **1985**, *C41*, 642.
(9) Gasperin, M. *Acta Crystallogr.* **1987**, *C43*, 1247.
(10) Gasperin, M. *Acta Crystallogr.* **1987**, *C43*, 2031.
(11) Gasperin, M. *Acta Crystallogr.* **1987**, *C43*, 2264.
(12) Gasperin, M. *Acta Crystallogr.* **1988**, *C44*, 415.
(13) Gasperin, M. *Acta Crystallogr.* **1989**, *C45*, 981.
(14) Gasperin, M. *Acta Crystallogr.* **1990**, *C46*, 372.
(15) Cousson, A.; Gasperin, M. *Acta Crystallogr.* **1991**, *C47*, 10.
(16) Wang, S.; Alekseev, E. V.; Diwu, J.; Casey, W. H.; Phillips, B. L.; Depmeier, W.; Albrecht-Schmitt, T. E. *Angew. Chem., Int. Ed.* **2010**, *49*, 1057.

(17) Yu, P.; Wang, S.; Alekseev, E. V.; Depmeier, W.; Albrecht-Schmitt, T. E.; Phillips, B.; Casey, W. *Angew. Chem., Int. Ed.* **2010**, *49*, 5975.
(18) Wang, S.; Alekseev, E. V.; Ling, J.; Liu, G.; Depmeier, W.; Albrecht-Schmitt, T. E. *Chem. Mater.* **2010**, *22*, 2155.
(19) Wang, S.; Alekseev, E. V.; Stritzinger, J. T.; Depmeier, W.; Albrecht-Schmitt, T. E. *Inorg. Chem.* **2010**, *49*, 2948.
(20) Wang, S.; Alekseev, E. V.; Stritzinger, J. T.; Depmeier, W.; Albrecht-Schmitt, T. E. *Inorg. Chem.* **2010**, *49*, 6690.
(21) Wang, S.; Alekseev, E. V.; Stritzinger, J. T.; Liu, G.; Depmeier, W.; Albrecht-Schmitt, T. E. *Chem. Mater.* **2010**, *22*, 5983.
(22) Wang, S.; Alekseev, E. V.; Ling, J.; Skanthakumar, S.; Soderholm, L.; Depmeier, W.; Albrecht-Schmitt, T. E. *Angew. Chem., Int. Ed.* **2010**, *49*, 1263.
(23) Wang, S.; Alekseev, E. V.; Depmeier, W.; Albrecht-Schmitt, T. E. *Chem. Commun.* **2010**, *46*, 3955.
(24) Wang, S.; Alekseev, E. V.; Miller, H. M.; Depmeier, W.; Albrecht-Schmitt, T. E. *Inorg. Chem.* **2010**, *49*, 9755.
(25) Bean, A. C.; Scott, B. L.; Albrecht-Schmitt, T. E.; Runde, W. *Inorg. Chem.* **2003**, *42*, 5632.
(26) Clark, D. L.; Hecker, S. S.; Jarvinen, G. D.; Neu, M. P. *The Chemistry of the Actinide and Transactinide Elements*; Springer: The Netherlands, 2006; Vol. 2, Chapter 7, pp 1108−1203.
(27) Bray, T. H.; Ling, J.; Choi, E. S.; Brooks, J. S.; Beitz, J. V.; Sykora, R. E.; Haire, R. G.; Stanbury, D. M.; Albrecht-Schmitt, T. E. *Inorg. Chem.* **2007**, *46*, 3663.
(28) Rao, L. *Chem. Soc. Rev.* **2007**, *36*, 881.
(29) Buhl, M.; Schreckenbach, G.; Sieffert, N.; Wipff, G. *Inorg. Chem.* **2009**, *48*, 9977.
(30) Hughes Kubatko, K.-A.; Helean, K. B.; Navrotsky, A.; Burns, P. C. *Science* **2003**, *302*, 1191.
(31) (a) Clark, D. L.; Hobart, D. E.; Neu, M. P. *Chem. Rev.* **1995**, *95*, 25. (b) Reilly, S. D.; Neu, M. P. *Inorg. Chem.* **2006**, *45*, 1839.
(32) Sheldrick, G. M. *SADABS 2001, Program for absorption correction using SMART CCD based on the method of Blessing*; Blessing, R. H. *Acta Crystallogr.* 1995, A51, 33
(33) Alcock, N. W.; Roberts, M. M.; Brown, D. *J. Chem. Soc., Dalton Trans.* **1982**, *1*, 33.
(34) Runde, W.; Bean, A. C.; Albrecht-Schmitt, T. E.; Scott, B. L. *Chem. Commun.* **2003**, *4*, 478.
(35) Apostolidis, C.; Schimmelpfennig, B.; Magnani, N.; Lindqvist-Reis, P.; Walter, O.; Sykora, R.; Morgenstern, A.; Colineau, E.; Caciuffo, R.; Klenze, R.; Haire, R. G.; Rebizant, J.; Bruchertseifer, F.; Fanghanel, T. *Angew. Chem., Int. Ed.* **2010**, *49*, 6343.
(36) Zachariasen, W. H. *J. Less-Common Met.* **1978**, *62*, 1.
(37) ICSD codes: (a) 51501: Fedoseev, A. M.; Budantseva, N. A.; Grigor'ev, M. S.; Bessonov, A. A.; Astafurova, L. N.; Lapitskaya, T. S.; Krupa, J. C. *Radiochim. Acta* **1999**, *86*, 17. (b) 93940: Andreev, G. B.; Antipin, M. Y.; Fedoseev, A. M.; Budantseva, N. A. *Kristallografiya* **2001**, *46*, 433. (c) 95921& 95922: Wang, J.; Kitazawa, T.; Nakada, M.; Yamashita, T.; Takeda, M. *Bull. Chem. Soc. Jpn.* **2002**, *75*, 253. (d) 98417: Fedosseev, A. M.; Budantseva, N. A.; Grigor'ev, M. S.; Guerman, K. E.; Krupa, J. C. *Radiochim. Acta* **2003**, *91*, 147. (e) 110324: Grigor'ev, M. S.; Tananaev, I. G.; Krot, N. N.; Yanovskii, A. I.; Struchkov, Y. T. *Radiokhimiya* **1997**, *39*, 323. (f) 157297& 157298& 157299& 157300: Forbes, T. Z.; Burns, P. C. *Can. Mineral.* **2007**, *45*, 471. (g) 173174: Talbot-Eeckelaers, C.; Pope, S. J. A.; Hynes, A. J.; Copping, R.; Jones, C. J.; Taylor, R. J.; Faulkner, S.; Sykes, D.; Livens, F. R.; May, I. *J. Am. Chem. Soc.* **2007**, *129*, 2442. (h) 173370: Bray, T. H.; Nelson, A. G. D.; Jin, G.; Haire, R. G.; Albrecht-Schmitt, T. E. *Inorg. Chem.* **2007**, *46*, 10959. (i) 201192: Alcock, N. W.; Roberts, M. M.; Brown, D. *J. Chem. Soc., Dalton Trans.* **1982**, *5*, 869. (j) 201232: Alcock, N. W.; Roberts, M. M.; Brown, D. *J. Chem. Soc., Dalton Trans.* **1982**, *1*, 33. (k) 250164: Grigor'ev, M. S.; Fedoseev, A. M.; Budantseva, N. A.; Bessonov, A. A.; Krupa, J. C. *Kristallografiya* **2004**, *49*, 676. (l) 281463 & 281464: Bean, A. C.; Scott, B. L.; Albrecht-Schmitt, T. E.; Runde, W. *Inorg. Chem.* **2003**, *42*, 5632. (m) Sykora, R. E.; Bean, A. C.; Scott, B. L.; Runde, W.; Albrecht-Schmitt, T. E. *J. Solid State Chem.* **2004**, *177*, 725. (n) 413331: Bean, A. C.; Scott, B. L.; Albrecht-Schmitt, T. E.; Runde, W. *J. Solid State Chem.* **2004**, *177*, 1346.
(38) Burns, P. C.; Ewing, R. C.; Hawthorne, F. C. *Can. Mineral.* **1997**, *35*, 1551.
(39) Brese, N. E.; O' Keeffe, M. *Acta Crystallogr.* **1991**, *B47*, 192.
(40) Liu, G.; Beitz, J. V. *The Chemistry of the Actinide and Transactinide Elements*; Springer: The Netherlands, 2006; Vol. 3, Chapter 18, pp 2013−2111.
(41) Friedman, H. A.; Toth, L. M. *J. Inorg. Nucl. Chem.* **1980**, *42*, 1347.
(42) Krot, N. N.; Grigoriev, M. S. *Russ. Chem. Rev.* **2004**, *73*, 89.
(43) Diwu, J.; Wang, S.; Liao, Z.; Burns, P. C.; Albrecht-Schmitt, T. E. *Inorg. Chem.* **2010**, *49*, 10074.
(44) Albrecht-Schmitt, T. E.; Almond, P. M.; Sykora, R. E. *Inorg. Chem.* **2003**, *42*, 3788.